

# A hybrid wavelength-mode division multiplexing-based inter-satellite optical wireless communication link

MEHTAB SINGH<sup>a,b</sup>, AMIT GROVER<sup>c</sup>, MEET KUMARI<sup>d,e</sup>, ANU SHEETAL<sup>f</sup>, REECHA SHARMA<sup>d</sup>, JYOTEESH MALHOTRA<sup>a</sup>

<sup>a</sup>Department of Engineering and Technology, Guru Nanak Dev University, Regional Campus, Jalandhar, India

<sup>b</sup>Department of ECE, Satyam Institute of Engineering and Technology, Amritsar (IKG-PTU, Kapurthala), India

<sup>c</sup>Department of ECE, Shaheed Bhagat Singh State University, Ferozepur, Punjab, India

<sup>d</sup>Department of ECE, Punjabi University, Patiala, Punjab, India

<sup>e</sup>Department of ECE, Chandigarh University, Punjab, India

<sup>f</sup>Department of Engineering and Technology, Guru Nanak Dev University, Regional Campus, Gurdaspur, India

In this work, a  $2\lambda \times 2$  spatial modes  $\times$  10 Gbps (40 Gbps) inter-satellite optical wireless communication (IsOWC) link has been proposed incorporating hybrid wavelength division multiplexing (WDM) and mode division multiplexing (MDM) techniques. The proposed link employs 2 distinct Hermite Gaussian (HG) spatial modes of 2 distinct wavelength channels (850 nm and 850.8 nm) to achieve a net data transmission rate of 40 Gbps. The link performance has been compared for non-return-to-zero (NRZ), return-to-zero (RZ), and alternate mark inversion (AMI) schemes. The proposed link demonstrates reliable transmission along 5000 km inter-satellite link with acceptable performance.

(Received November 14, 2020; accepted October 7, 2021)

**Keywords:** IsOWC, MDM, WDM, HG modes

## 1. Introduction

Optical wireless communication (OWC) based inter-satellite OWC (IsOWC) uses laser technology to send data between two satellite terminals separated by outer-space channel. IsOWC has obtained significant importance over conventional microwave links due to its many advantages such as low power requirement, light weight terminals, high-speed transmission, secure communication, narrow beam divergence and fast deployment. The performance of an IsOWC system depends on factors such as transmission power, operating wavelength, pointing error angle, modulation, and coding etc. The essential condition for a feasible IsOWC link is establishing a line-of-sight (LOS) formation between the transmitter and receiver terminals. Any LOS configuration misalignment may lead to received signal quality deterioration and causes link failure, which is also referred as pointing error angle loss. The primary reasons for these errors are mechanical vibrations, electronic disturbances as well as platform jitter [1,2]. IsOWC technology is primarily utilized for information relaying between satellites in same or different orbits with data transmission at the speed of light [3,4]. I. Aggarwal et al. demonstrates that as the aperture diameter and transmitted power increases, the IsOWC link performance improves up to 5000 km link distance at 5.6 Gbps [5]. S. Kumar et al. in [6] proposed a non-return-to-zero (NRZ) subcarrier multiplexing (SCM) based IsOWC link and reported 1.8 Gbps transmission along 5000 km

range at 850 nm, 1064 nm, and 1550 nm wavelength. S. Ganga et al. in [7] reported a low-power IsOWC link employing square root module (SRM) for improved link performance. Further, the authors reported comparison of different electrical filters for optimal link performance. 2.5 Gbps information was successfully transported at 5000 km IsOWC range. S. Pradhan et al. reported the comparative performance analysis of IsOWC link using return-to-zero (RZ) modulated Mach Zehnder modulator (MZM) and LiNbO<sub>3</sub> modulators for 16-channels each at 5Gbps-100 km range and a superior performance of MZM than LiNbO<sub>3</sub> modulator is reported [8]. Several researchers have investigated the impact of different modulation schemes such as NRZ, RZ, on-off keying (OOK), etc. on IsOWC links covering limited distance up to tens of km. Currently wavelength division multiplexing (WDM) technology has witnessed a significant interest in enhanced bandwidth capacity for IsOWC links. WDM technology transmits information from multiple sources over a single transmission link while supporting the signals on separate wavelengths [3,9,10].

Further, mode division multiplexing (MDM) offers parallel data transmission using different modes. It provides a new multiplexing dimension for multiple information channels transmission via a single IsOWC link besides of intensity, wavelength, phase, time and polarization [11]. Mode types employed in MDM can be donut, Laguerre-Gaussian (LG), and the most efficient Hermite-Gaussian (HG) modes [12–14]. A. Sharma et al.

in [15] proposed and investigated a 20 Gbps NRZ-MDM modulated signal transmission over IsOWC link range of 1600 km incorporating LG00 and LG01 modes. P.K. Jha et al. in [16] reported an enhanced performance analysis of an M-ary quadrature amplitude modulation (QAM) based multi-input single output (MISO)-FSO transmission system utilizing spatial diversity and multi-hop relay under the impact of different weather conditions, atmospheric turbulence and geometric losses at the source. H.T.T. Pham et al. in [17] investigated the performance of an M-ary pulse-position modulation (PPM) based FSO transmission system under the impact of atmospheric turbulence and misalignment fading by employing partially-coherent Gaussian-beam model. E.E. Elsayed et al. in [18] reported enhanced performance analysis of an eight-channel WDM-passive optical network based on hybrid fiber-FSO transmission at 2.5 Gbps data rate utilizing OOK modulation under the impact of varying atmospheric turbulence conditions. The numerical results show that the proposed system improves the signal to noise ratio (SNR) and power penalty at  $10^{-12}$  BER. A.A. Farid et al. in [19] reported the designing and performance analysis of a FSO communication link with optimized outage capacity under the combined effect of pointing errors and turbulence taking into consideration beam width, jitter variance, and detector size. M. Singh et al. in [20] reported simulative analysis of a 20 Gbps OFDM-FSO transmission system using different HG modes over 50 km transmission range. M. Singh et al. in [21] reported performance evaluation of a MDM based radio over FSO (RoFSO) link using RZ, NRZ, and differential phase shift keying (DPSK) modulation formats under varying Gamma-Gamma turbulent conditions and atmospheric weather. M. Abaza et al. in [22] reported improved performance of a MISO-based FSO system by employing multi-hop decode and forward relaying as compared to direct link under the impact of log-normal turbulent channel with different weather conditions and geometric losses. E. E. Elsayed et al. in [23] proposed and analytically investigated a novel MISO-FSO transmission system employing aperture averaging and spatial-coherence diversity technique with modified-pulse position modulation to enhance the spectral efficiency of the link. D. Anandkumar et al. in [24] reported a comprehensive literature survey on different modulation and multiplexing techniques reported in literature for improving the BER and SNR performance of FSO transmission links under atmospheric weather and turbulence conditions. Further, the authors reported various channel models that impact the availability of FSO links. Y. Zhang et al. in [25] reported multi-input multi-output (MIMO)-FSO transmission employing multiple PPM under the influence of pointing errors and uncorrelated fading conditions. Further, the authors reported that by using pointing, acquisition, and tracking

techniques, the performance of FSO system under the impact of turbulence and pointing errors can be improved. A.A. Algamal et al. in [26] investigated the performance of a FSO link over Alexandria city in Egypt taking into consideration pointing errors, atmospheric turbulence, operating wavelength, type of photodetector, modulation format, thermal noise, background noise, and antenna aperture size. The authors demonstrated that the proposed FSO link can be employed for providing a wide range of services to end terminal users. A.K. Rahman et al. in [27] proposed dual diffuser modulation (DDM) based FSO system and compared its performance with conventional OOK modulation. The authors reported that by employing the proposed DDM, significant improvement in the received power and threshold level of signal under the effect of atmospheric turbulence is observed. S. Chaudhary et al. in [28] proposed the modelling and performance analysis of a mode-wavelength division multiplexing (MWDM) based RoFSO system employing photonic crystal fiber based mode multiplexer and demultiplexers. M. Singh et al. in [29] investigates the performance of an underwater wireless optical communication (UWOC) system under the impact of distinct sizes of air bubbles. H. Lei et al. in [30] investigates the secrecy outage probability of a hybrid RF-FSO transmission system under the influence of pointing errors, atmospheric turbulence, path loss, and energy harvesting. M. Uysal et al. in [31] discussed in detail an overview, range of applications and merits of OWC technology in comparison to conventional RF transmission systems. M. Lavery et al. in [32] reported the detection mechanism of a spinning object by analysing the orbital angular momentum (OAM) of light beam emitted from the object for the purpose of implementing remote detection of astronomical and terrestrial settings. K. Liu et al. in [33] reported the application of passive-OAM technique for radar imaging and demonstrated that the proposed system providing significant robustness against noise influence as compared to active-OAM technique for radar imaging. M. Barbuto et al. in [34] reported the designing of a novel circular patch antenna capable of exciting distinct right-handed circularly polarized modes, which can be deployed for increasing information transmission rates in mobile and satellite communication systems. N. Zhao et al. in [35] introduced the concept of OAM multiplexing to improve the capacity in FSO transmission link. Further, the authors demonstrated that OAM transmission outperformed both conventional LOS-MIMO transmission and spatial multiplexing. D. Miller in [36] discussed optimal choices other than OAM multiplexing for communication systems including prolate spheroidal function and singular-value decomposition of coupling operator between transmitter and receiver spaces. M. Oldoni et al. in [37] discussed the impact of size and position of transmitter and receiver antenna in an OAM transmission in MIMO based RF

system. J. Xu et al. in [38] discussed the dependency of degree of freedom of OAM transmission on the link distance between the transmitter and the receiver terminal. D. Nguyen et al. in [39] reported performance of a circular array of antenna to transmit OAM beam for telecommunication applications. Further, the link budget of the proposed RF transmission system is analysed using commercially available simulation software. P. Vaveliuk et al. in [40] validates the paraxiality of Bessel-Gaussian, Hermite, and Laguerre beams by employing integral criteria based on paraxial wave equations. B. Yousif et al. in [41] reported a novel RF-FSO transmission system employing hybrid MIMO-MDM techniques with M-ary PPM and spatial PPM to enhance the channel transmission capacity. The authors further reported that by increasing the transmitter and receiver antenna aperture diameter to 8 cm and 10 cm, the performance of the proposed link under the impact of weak and strong turbulence conditions improves. H. Huang et al. in [42] have reported the designing of an OAM mode sorter with high mode selectivity of -15 dB. As a proof of concept, the authors reported transportation of two independent 20 Gbps polarization division multiplexed-quadrature phase-shift

keyed data streams over 5 km few-mode graded-indexed fiber with MIMO digital signal processing for eliminating inter-channel crosstalk.

In this paper, we propose and investigate a 40 Gbps IsOWC link employing hybrid NRZ/RZ/alternate mark inversion (AMI)-WDM-MDM transmission with two distinct HG spatial modes over 5000 km transmission distance. The performance of the proposed system has been analyzed using Optisystem simulation software. This paper is organized as- Section 2 depicts the system design of the proposed hybrid NRZ/RZ/AMI-WDM-MDM-IsOWC transmission link. Section 3 discusses the simulation results and the conclusion is drawn in Section 4.

## 2. System design

In proposed work, Optisystem v.15 simulation software is used to design and investigate the hybrid WDM-MDM-IsOWC system incorporating two distinct HG spatial modes viz. HG00 and HG01. Fig. 1 illustrates the diagram of the proposed system.

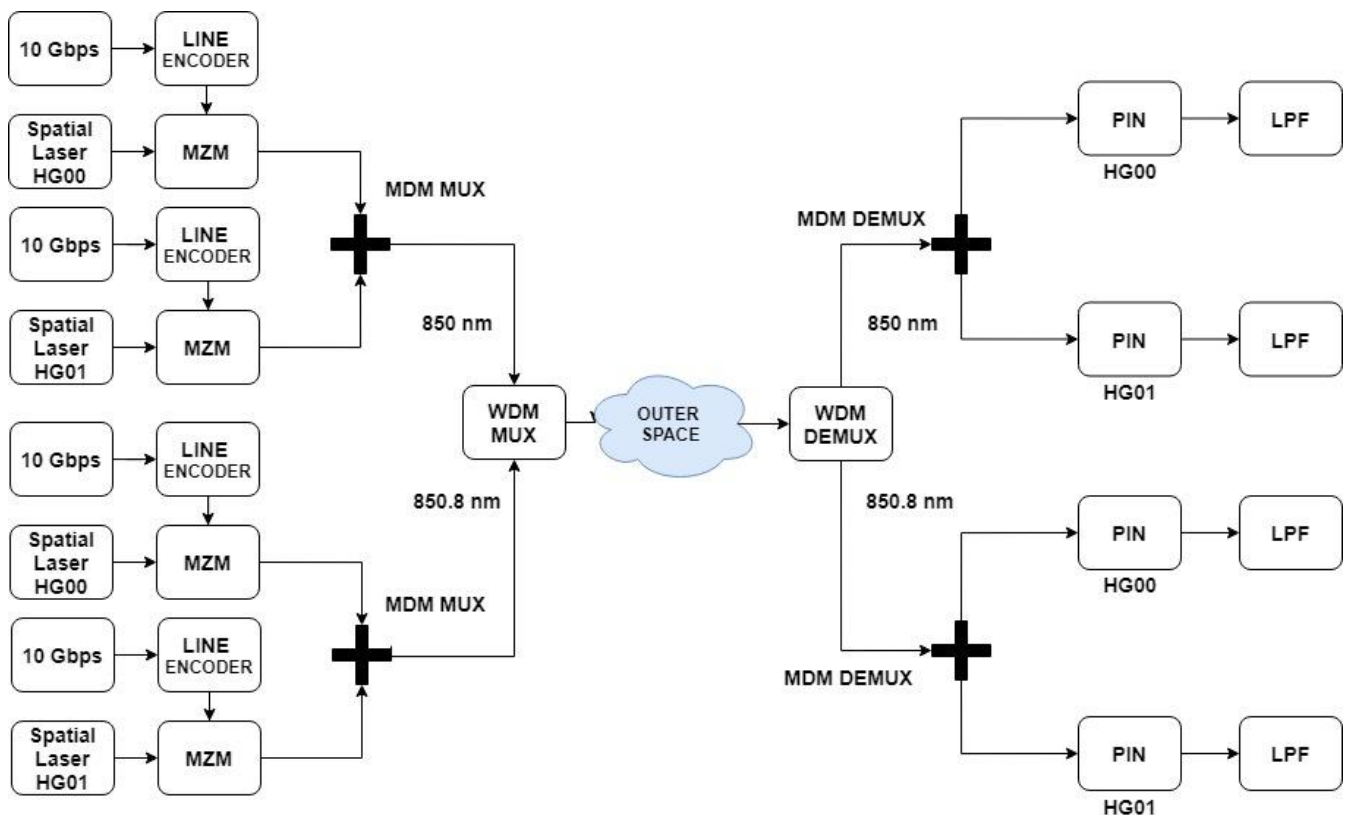


Fig. 1. Schematic of the proposed WDM-MDM-IsOWC Link

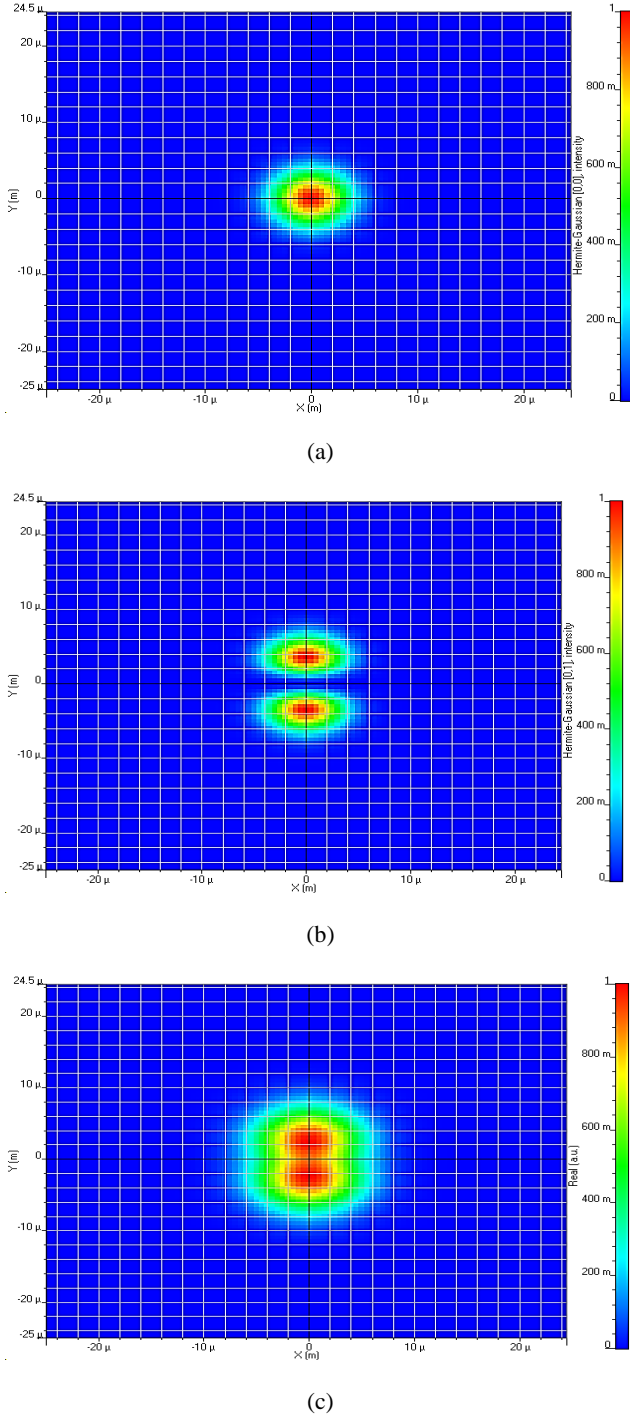


Fig. 2. Spatial profiles of (a) HG00 (b) HG01 (c) HG00+HG01 (after MDM MUX) (color online)

Two distinct NRZ, RZ and AMI line encoded signals each transporting 10 Gbps data are simultaneously transferred over HG00 and HG01 modes at operating wavelength of 850 nm. Likewise, another two encoded signals are transmitted over 850.8 nm wavelength. HG modes can be expressed as [43,44]:

$$\Phi_{a,b}(x,y) = H_a\left(\frac{\sqrt{2}x}{\omega_{0,x}}\right) \exp\left(-\frac{x^2}{\omega_{0,x}^2}\right) \exp\left(j\frac{\pi x^2}{\lambda R_{0,x}}\right) H_b\left(\frac{\sqrt{2}y}{\omega_{0,y}}\right) \exp\left(-\frac{y^2}{\omega_{0,y}^2}\right) \exp\left(j\frac{\pi y^2}{\lambda R_{0,y}}\right) \quad (1)$$

where  $x$  and  $y$  denote the mode dependencies on X- and Y-polarization axis respectively,  $R$  is the curvature radius,  $\omega_0$  presents spot size and  $H_x$  and  $H_y$  represent the Hermite polynomials. For generating two independent HG00 and HG01 modes at central wavelength of 850 nm, spatial continuous wave (CW) laser along with multi-mode generator is used. Fig. 2 depicts the spatial profiles of excited modes. 10 Gbps binary information per spatial laser is generated using a Pseudo-random bit sequence generator (PRBS) and is further line encoded by employing a NRZ, RZ or AMI encoder and then directed towards a MZM [45–48]. After the MZM modulation of the input signal over an optical carrier signal of 850 nm wavelength, both output MZM signals are combined using an MDM multiplexer (MUX). Similarly, two independent HG00 and HG01 modes using different line encoders at 850.8 nm wavelength are modulated and combined using another MDM MUX. The modulated signals from both the MDM MUX are combined using WDM MUX and then transmitted over FSO channel [49,50]. The optical spectra of the transmitted signal after WDM MUX for NRZ, AMI and RZ modulation is depicted in Fig 3(a), (b) and (c) respectively. At the receiver side, 850 nm and 850.8 nm wavelengths channels are separated using a WDM demultiplexer (DEMUX) followed by two MDM DEMUX. For each signal detection, a PIN photodiode is used to recover the received signal, a low pass filter (LPF) is used to reduce the noise and to attain a high quality signal and a BER analyser is used for analysing the signal performance [51-53]. The signal quality is analyzed through a BER analyser in terms of BER and eye diagrams. Table 1 presents the simulation parameters used in this work.

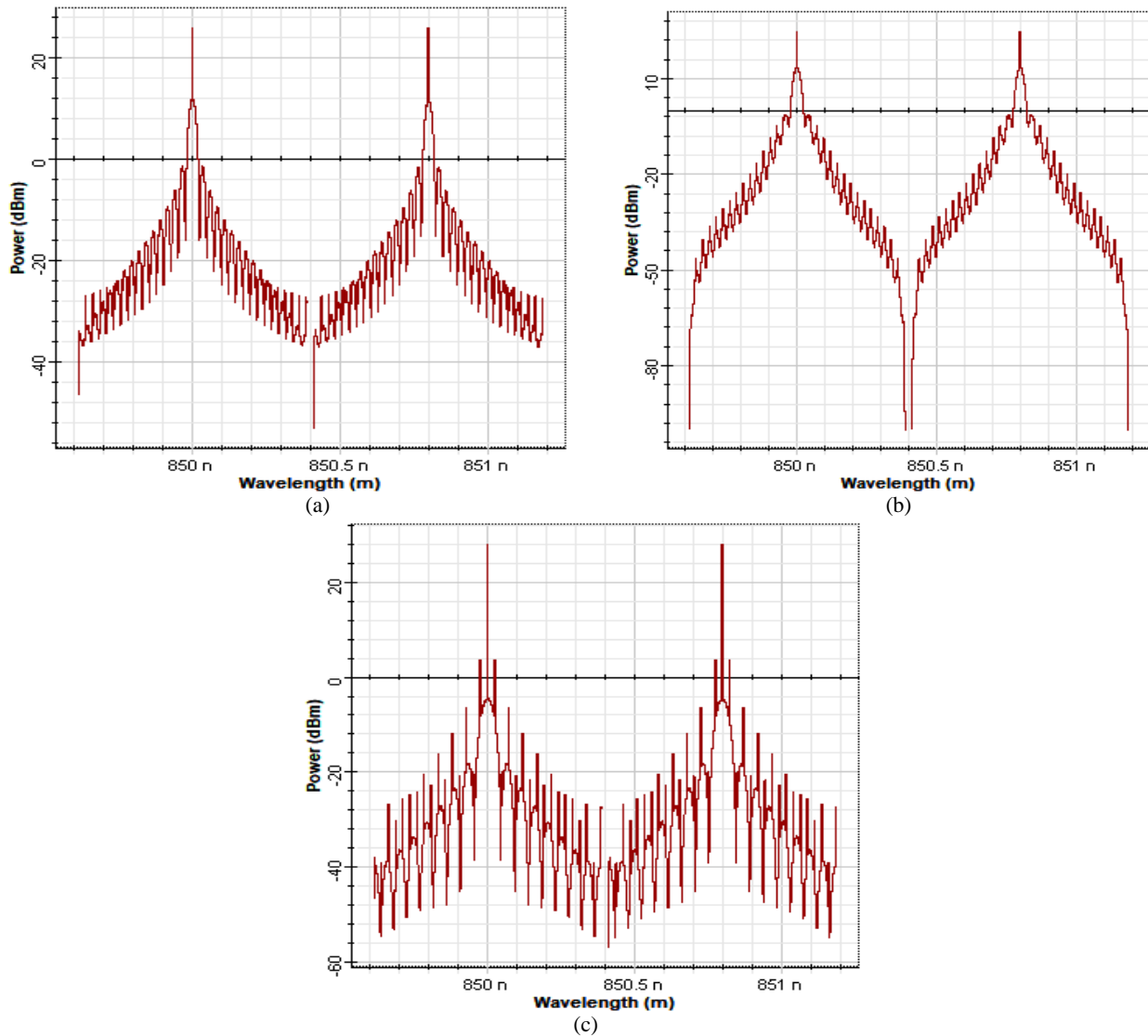


Fig. 3. Optical spectrum of the transmitted signal (after WDM MUX) (a) NRZ modulation (b) AMI modulation (c) RZ modulation

Table 1. Simulation parameters [54, 55]

Parameters	Values
Operating wavelength	850 nm and 850.8 nm
Channel spacing	0.8 nm
Bit rate/channel	10 Gbps
CW Laser line width	0.1 MHz
CW Laser power	30 dBm
MZM extinction ratio	30 dB
Atmospheric attenuation	0 dB/km
Transmitter aperture diameter	15 cm
Receiver aperture diameter	15 cm
WDM MUX/DEMUX bandwidth	10 GHz
Transmitter optics efficiency	80%
Receiver optics efficiency	80%
Receiver pointing error angle	1.1 $\mu$ rad
Transmitter pointing error angle	1.1 $\mu$ rad
PIN photodiode responsivity	1 A/W
Sequence Length	1024
Samples per bit	32
Additional losses due to background noise radiations and platform jitters	5 dB

### 3. Results and discussion

Fig. 4 shows the performance comparison of the IsOWC link based on hybrid WDM-MDM system for 850 nm and 850.8 nm using NRZ, RZ and AMI modulation

formats. Here, 1.1  $\mu$ rad pointing error angle is considered and the results are computed in terms of log of BER as performance metrics over 4000-5000 km transmission range.

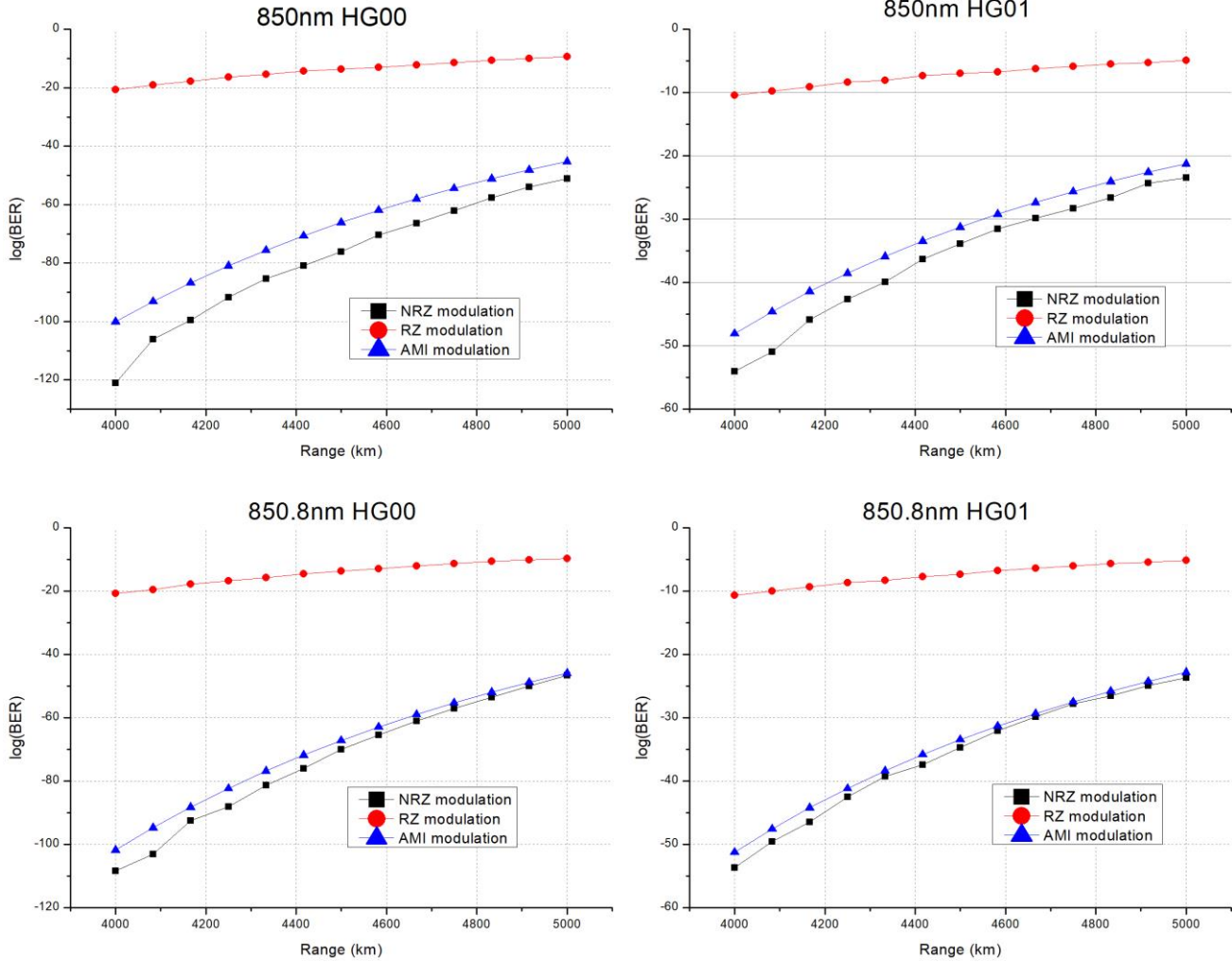
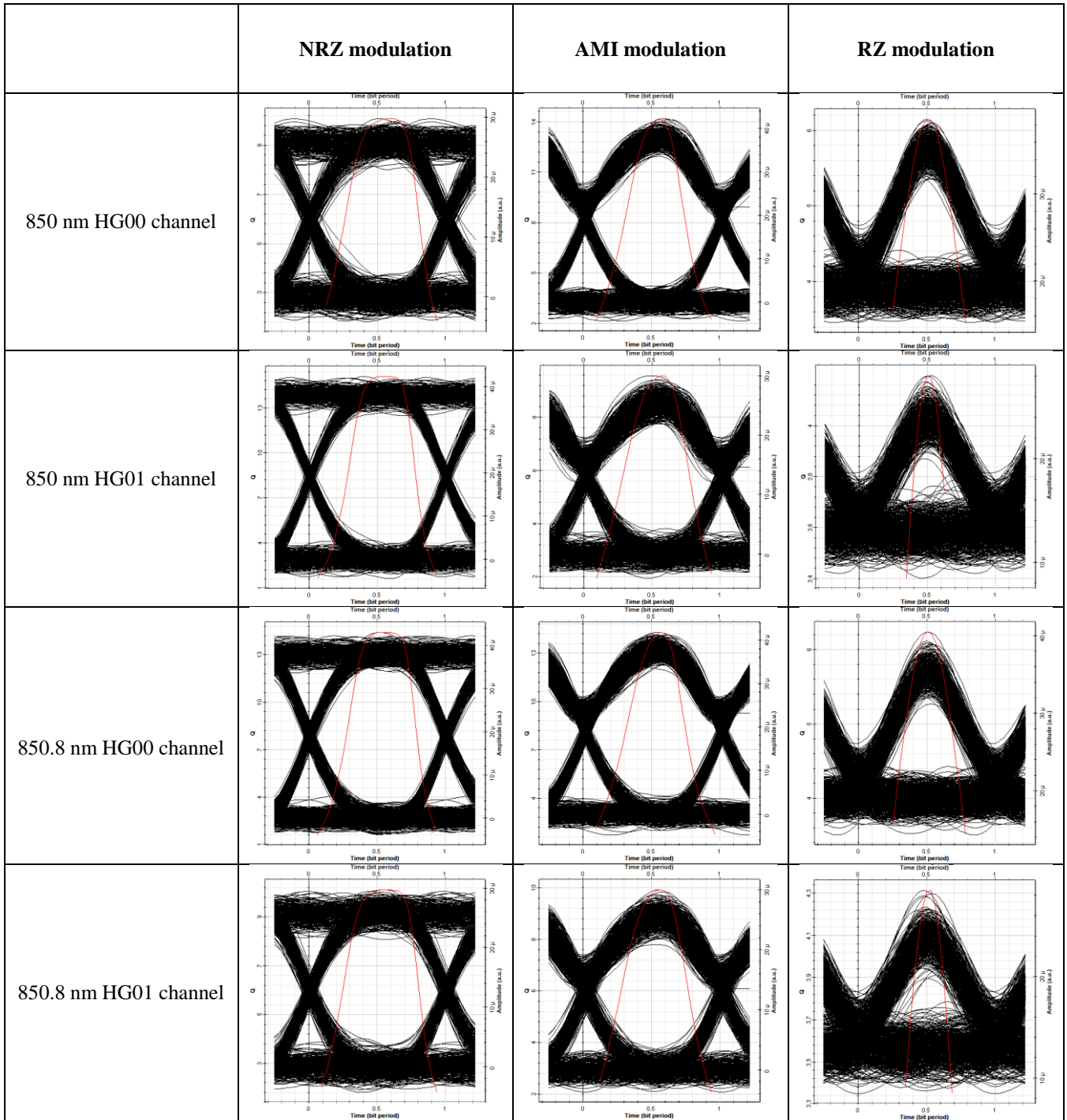


Fig. 4. Log(BER) versus IsOWC range (color online)

From the obtained results, it can be depicted that the log of BER of the received signal for HG00 mode channel at 850 nm wavelength for NRZ, RZ and AMI modulation is computed as -51.10, -9.40 and -45.24 respectively at a IsOWC range of 5000 km. Also, for HG01 mode channel at 850 nm wavelength, the log of BER of the received signal for NRZ, RZ and AMI modulation is determined as -23.46, -4.87 and -21.23 respectively at 5000 km IsOWC range. Similarly at 5000 km IsOWC range, for HG00 and HG01 mode channels, the log of BER of the received signal for NRZ, RZ and AMI modulation is determined as -46.62 and -23.64; -9.66 and -5.09; and -45.89 and -22.79 at 850.8 nm wavelength respectively. The results illustrate

that with the rise in transmission range, the performance of the system degrades. Also, the computed results report that the performance of HG00 mode is considerably better than HG01 and NRZ modulation performs the best by providing reliable 40 Gbps transmission along 5000 km IsOWC range, followed by AMI and RZ modulation scheme. Table 2 presents the eye diagrams of the recovered data signals at the user end for all three modulations formats and validates the above discussion.

Table 2. Eye diagrams of the received signals at 5000 km IsOWC range



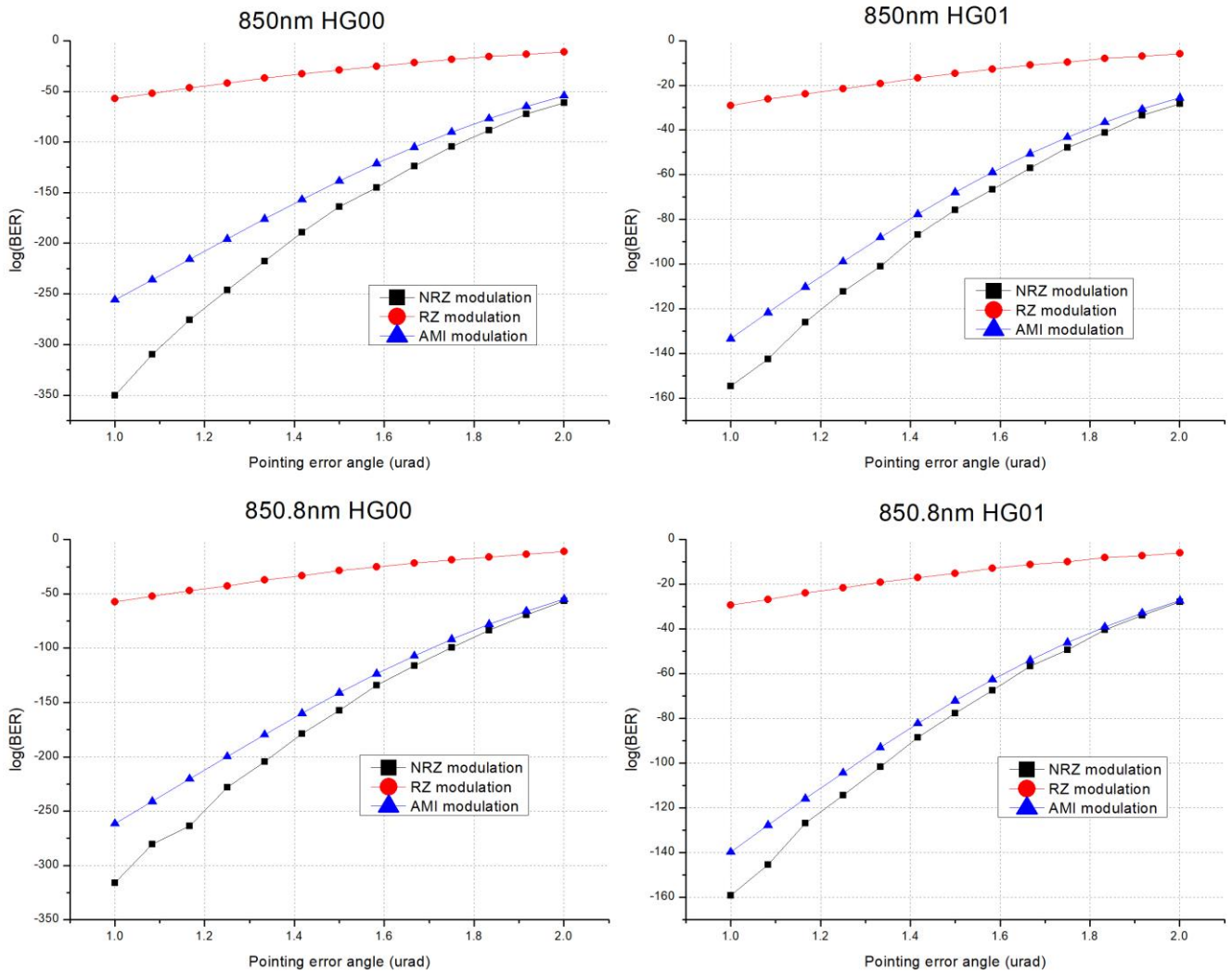


Fig. 5. Log(BER) versus pointing error angle (color online)

Further, we analyzed the impact of pointing error angle on the proposed link performance over 4000 km IsOWC link range. Fig. 5 depicts that with the rise in pointing error angle, the system performance deteriorates. From Fig. 5 it is noted that log of BER of the received signal for HG00 and HG01 mode channels operating at 850 nm wavelength is measured as -61.03 and -28.17 for NRZ; -11.15 and -5.84 for RZ and -54.14 and -25.48 for AMI modulation respectively at pointing error angle of 2.0  $\mu\text{rad}$ . Similarly, log of BER for HG00 and HG01 mode

channels operating at 850.8 nm wavelength is measured as -56.62 and -27.80 for NRZ; -11.12 and -5.91 for RZ and -54.95 and -27.31 for AMI modulation respectively. The successful transmission range under 2.0  $\mu\text{rad}$  pointing error angle impact is 4000 km for 4 $\times$ 10 Gbps data transmission using HG00 and HG01 mode channel at two different wavelengths of 850 nm and 850.8 nm. Table 3 represents the eye diagram of the recovered data signals at the user end for all three modulations formats and validates the above discussion.

Table 3. Eye diagrams at 2  $\mu$ rad pointing error angle

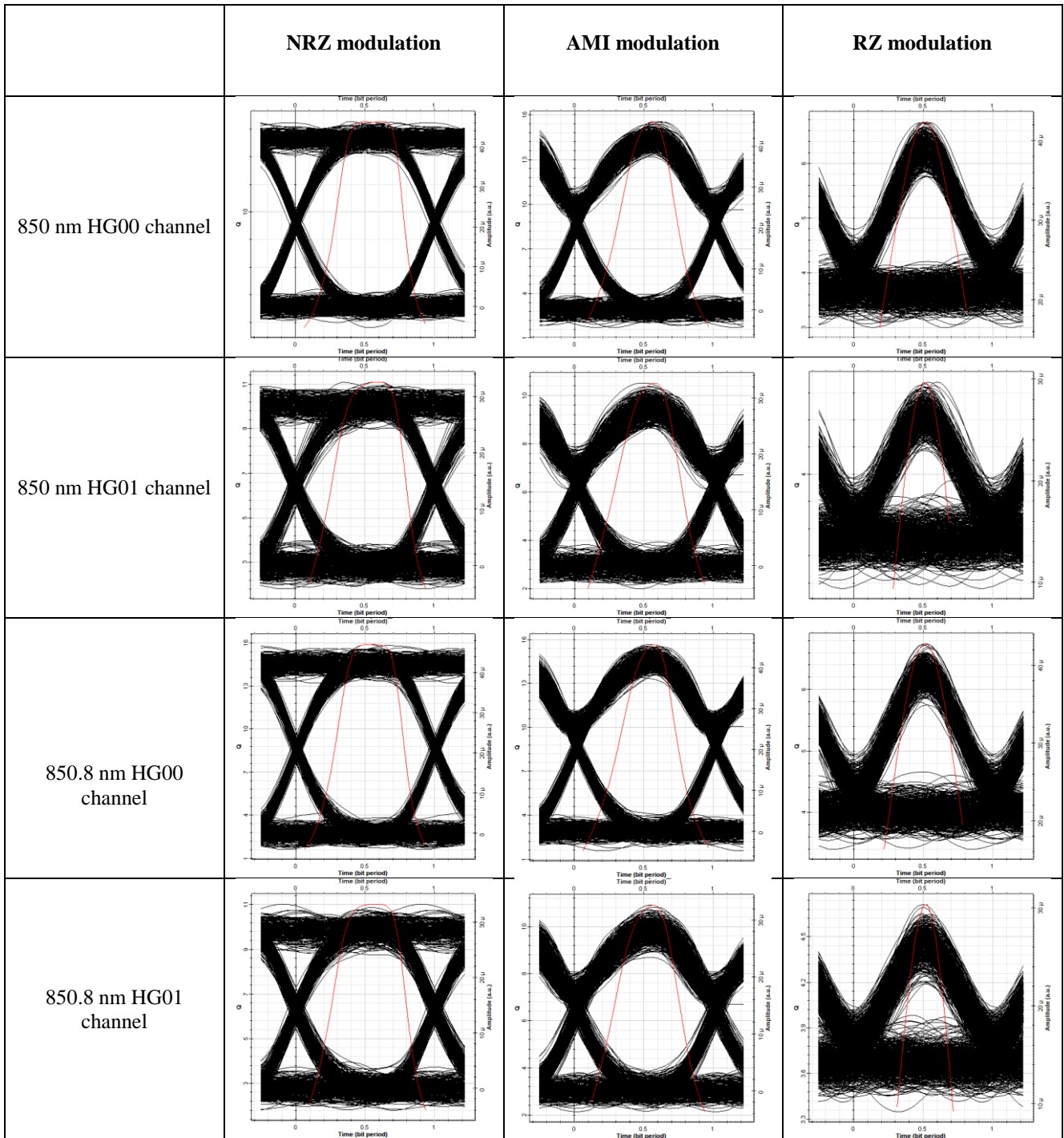


Table 4 compares the performance of the proposed IsOWC link with reported works in the literature and from the comparative analysis it can be seen that the proposed

IsOWC solution provides higher data transmission rates as compared to existing works.

Table 4. Comparison of the proposed IsOWC link performance with existing works

Authors, Reference	Journal, Year	Technique	Data rate	Coverage range
S. Kumar, Ref [6]	Wireless Personal Communication, 2018	NRZ-SCM transmission	1.8 Gbps	5000 km
S. Ganga, Ref [7]	Procedia Technology, Elsevier, 2016	Single-channel NRZ transmission with SRm detection	2.5 Gbps	5000 km
S. Sharma, Ref [15]	Optik, Elsevier, 2020	NRZ-LG-MDM transmission	20 Gbps	1600 km
Proposed work	-	NRZ-WDM-MDM transmission	40 Gbps	5000 km

#### 4. Conclusion

In this work, the designing of a 4×10 Gbps hybrid WDM-MDM based IsOWC link employing HG00 and HG01 modes using different modulation formats is reported. Further, the proposed IsOWC link performance is analyzed under the impact of varying pointing error angle and increasing range for 850 nm and 850.8 nm operating wavelengths. The results presented report that HG00 mode performs better than HG01 mode over the IsOWC link. Also, NRZ modulation performs the best in terms of BER of the received signal, followed by AMI and RZ modulation format. The proposed link demonstrates faithful 40 Gbps transmission along 5000 km IsOWC range under 1.1  $\mu$ rad pointing error angle whereas the IsOWC range is limited to 4000 km under 2  $\mu$ rad pointing error angle. The proposed IsOWC link performance is also compared with reported works in the literature and the comparison shows that the proposed link demonstrates higher IsOWC transmission rate. In future works, the transmission capacity of the proposed link can be further improved by incorporating more number of spatial channels and by employing hybrid polarization division multiplexing technique along with WDM and MDM systems. Further, the proposed system can be used for high-speed transmission applications such as big data, cloud computing, artificial intelligence, and Internet of Things (IoT) etc.

#### References

- [1] P. Sivakumar, M. Singh, J. Malhotra, V. Dhasarathan, *Wirel. Networks* **26**, 3579 (2020).
- [2] G. Kumari, C. Selwal, *Int. Conf. Signal Process. Commun. Power Embed. Syst. SCOPES 2016 - Proc. 1800* (2017).
- [3] A. A. Shatnawi, M. N. Bin Mohd Warip, A. M. Safar, *J. Opt. Commun.* **39**, 123 (2017).
- [4] S. Singh, H. Kaur, *Comput. Sci. Syst. Eng. Eff.* **12**, 299 (2016).
- [5] I. Aggarwal, P. Chawla, R. Gupta, *Adv. Electron. Electr. Eng.* **3**, 847 (2013).
- [6] S. Kumar, S. S. Gill, K. Singh, *Wireless Personal Communication* **98**, 1461 (2018).
- [7] S. Ganga, R. S. Asha, P. J. Shaija, *Procedia Technology* **25**, 567 (2016).
- [8] S. Pradhan, G. Sagarika, S. Patnayak, M. R. Nilarout, *Abhyantri* **4**(4), 36 (2017).
- [9] V. Sharma, A. Kaur, *Proc. of International Conference on Advances in Communication, Network and Computing* **1**, 52 (2013).
- [10] N. Kaur, G. Soni, *Int. J. Sci. Res. Publ.* **5**, 1 (2015).
- [11] M. Singh, J. Malhotra, *Wirel. Pers. Commun.* **111**, 495 (2020).
- [12] A. Amphawan, Y. Fazea, H. Ibrahim, *Int. Conf. Opt. Photonic Eng. (IcOPEN 2015)* **9524**, 95240S (2015).
- [13] M. Singh, J. Malhotra, *Wirel. Pers. Commun.* **107**, 1549 (2019).
- [14] S. Chaudhary, B. Lin, X. Tang, X. Wei, Z. Zhou, C. Lin, M. Zhang, H. Zhang, *Opt. Quantum Electron.* **50**, 1 (2018).
- [15] A. Sharma, V. K. Thapa, B. Sharma, *Optik* **227**, 165250 (2020).
- [16] Pranav J. Kumar, Kalyani K. Nitin, K. Kumar, 4th International Conference on Electrical Energy Systems (ICEES), SSNCE, Chennai, TN, India, 8442405, 9 (2018).
- [17] H. T. Pham, N. T. Dang, A. T. Pham, *IET Communications* **8**(10), 1762 (2014).
- [18] E. E. Elsayed, B. B. Yousif, *Opt. Quantum Electron.* **50**(7), 1 (2008).
- [19] A. A. Farid, S. Hranilovic, S., *Journal of Lightwave Technology* **25**(7), 1702 (2007).
- [20] M. Singh, J. Malhotra, *Wireless Personal Communications* **107**, 1549 (2019).
- [21] M. Singh, J. Malhotra, *Optical Engineering* **58**(4), 046112 (2019).
- [22] M. Abaza, R. Mesleh, A. Mansour et. al., *Optics Communications* **334**, 247 (2015).
- [23] E. E. Elsayed, B. B. Yousif, *Optics Communications* **463**, 125463 (2020).
- [24] D. Anandkumar, R. G. Sangeetha, *Opt. Quantum Electron.* **53**, 5-1 (2021).
- [25] Y. Zhang, H. Wang, M. Cao, Z. Bao, *Int. J. Antennas Propag.* **2020**, 7083812-1 (2020).
- [26] A. A. Algarni, H. A. Fayed, M. Mahmoud, M. H. Aly, *Opt. Quantum Electron.* **52**(7), 349-1 (2020).
- [27] A. K. Rahman et. al., *IOP Conf. Ser. Mater. Sci. Eng.* **767**(1), 012035-1 (2020).
- [28] A. Amphawan, S. Chaudhary, Z. Ghassemlooy, T. K. Neo, *Opt. Commun.* **467**, 125539-1 (2020).

- [29] M. Singh, M. L. Singh, G. Singh, H. Kaur, Priyanka, S. Kaur, *Opt. Quantum Electron.* **52**(12), 515-1 (2020).
- [30] H. Lei, Z. Dai, K. H. Park, W. Lei, G. Pan, M. S. Alouini, *IEEE Trans. Commun.* **66**(12), 6384 (2018).
- [31] M. Uysal, H. Nouri, *Int. Conf. Transparent Opt. Networks* pp. 1-7 (2014).
- [32] M. P. J. Lavery et. al., *Science* **341**(6145), 537 (2013).
- [33] K. Liu, Y. Cheng, X. Li, Y. Jiang, *IEEE Microwave and Wireless Components Letters* **28**(9), 840 (2018).
- [34] M. Barbuto, M. Miri, A. Alù, F. Bilotti, A. Toscano, *IEEE Transactions on Antennas and Propagation* **68**(3), 1851 (2020).
- [35] N. Zhao, X. Li, G. Li, J. M. Kahn, *Nature Photonics* **9**, 822 (2015).
- [36] D. A. B. Miller, *Proceedings of the National Academy of Sciences* **114**(46), E9755 (2017).
- [37] M. Oldoni et al., *IEEE Transactions on Antennas and Propagation* **63**(10), 4582 (2015).
- [38] J. Xu et. al., *IEEE Trans. Antenna Prop.* **65**, 4 (2017).
- [39] D. K. Nguyen et al., *Radio Science* **50**(11), 1165 (2015).
- [40] P. Vaveliuk, B. Ruiz, A. Lencina, *Optics Letters* **32**(8), 927 (2007).
- [41] B. Yousif Bedir, E. Elsayed Ebrahim, M. Alzalabani Mahmoud, *Opt. Commun.* **436**, 197 (2019).
- [42] H. Huang et al., *Scientific Reports* **5**(1), 1 (2015).
- [43] M. Singh, J. Malhotra, *J. Opt. Commun.* **40**(3), 295 (2019).
- [44] A. Amphawan, S. Chaudhary, R. Din, M. N. Omar, *Proc. - 2015 IEEE 11th Int. Colloq. Signal Process. its Appl. CSPA 2015* 145 (2015)
- [45] Z. Zhou, E. Li, H. Zhang, *J. Opt. Commun.* **10**(1) (2019).
- [46] S. Chaudhary, A. Amphawan, N. Ali, M. S. Sajat, *4th Int. Conf. Internet Appl. Protoc. Serv.* **4**, 241 (2015).
- [47] V. Sharma, R. Kaur, *Optik* **124**(17), 3112 (2013).
- [48] P. Sharma, *Int. J. Eng. Res. Technol.* **7**, 261 (2018).
- [49] M. Singh, J. Malhotra, V. Dhasarathan, *Microw. Opt. Technol. Lett.* **62**, 4007 (2020).
- [50] S. Chaudhary, X. Tang, A. Sharma, B. Lin, X. Wei, A. Parmar, *Opt. Quantum Electron.* **51**, 1 (2019).
- [51] I. B. Djordjevic, *Adv. Opt. Wirel. Commun. Syst.* **2**, 1 (2017)
- [52] A. Bhowal, Anirban, R. S. Kshetrimayum, *Signals and Communication Technology* **1**, 22 (2021).
- [53] B. Kumbhani, R. S. Kshetrimayum, *MIMO Wirel. Commun. over Gen. Fading Channels* **1**, 1 (2017).
- [54] A. Grover, A. Sheetal, *Wireless Personal Communication* **114**(3), 2449 (2020).
- [55] B. Patnaik, P. K. Sahu, *IET Communications* **6**(16), 2561 (2012).

---

\*Corresponding author: mehtab91singh@gmail.com